# Growth Hormone Secretagogues Exert Differential Effects on Skeletal Muscle Calcium Homeostasis in Male Rats Depending on the Peptidyl/Nonpeptidyl Structure

Antonella Liantonio, Gianluca Gramegna, Giuseppe Carbonara, Valeriana Teresa Sblendorio, Sabata Pierno, Bodvaël Fraysse, Viviana Giannuzzi, Laura Rizzi, Antonio Torsello, and Diana Conte Camerino

Section of Pharmacology (A.L., G.G., G.C., V.T.S., S.P., V.G., D.C.C.), Department of Pharmacy-Drug Sciences, University of Bari, Campus, 70125 Bari, Italy; Physiopathologie Animale et bioThérapie du muscle et du système nerveux (B.F.), Ecole Nationale Vétérinaire, Agroalimentaire et de l'Alimentation, Nantes-Atlantique, 44307 Nantes Cedex 03, France; and Department of Health Sciences (L.R., A.T.), University of Milano-Bicocca, 20900 Monza, Italy

The orexigenic and anabolic effects induced by ghrelin and the synthetic GH secretagogues (GHSs) are thought to positively contribute to therapeutic approaches and the adjunct treatment of a number of diseases associated with muscle wasting such as cachexia and sarcopenia. However, many questions about the potential utility and safety of GHSs in both therapy and skeletal muscle function remain unanswered. By using fura-2 cytofluorimetric technique, we determined the acute effects of ghrelin, as well as of peptidyl and nonpeptidyl synthetic GHSs on calcium homeostasis, a critical biomarker of muscle function, in isolated tendon-to-tendon male rat skeletal muscle fibers. The synthetic nonpeptidyl GHSs, but not peptidyl ghrelin and hexarelin, were able to significantly increase resting cytosolic calcium $[Ca^{2+}]_i$. The nonpeptidyl GHS-induced $[Ca^{2+}]_i$ increase was independent of GHS-receptor 1a but was antagonized by both thapsigargin/caffeine and cyclosporine A, indicating the involvement of the sarcoplasmic reticulum and mitochondria. Evaluation of the effects of a pseudopeptidyl GHS and a nonpeptidyl antagonist of the GHS-receptor 1a together with a drug-modeling study suggest the conclusion that the lipophilic nonpeptidyl structure of the tested compounds is the key chemical feature crucial for the GHS-induced calcium alterations in the skeletal muscle. Thus, synthetic GHSs can have different effects on skeletal muscle fibers depending on their molecular structures. The calcium homeostasis dysregulation specifically induced by the nonpeptidyl GHSs used in this study could potentially counteract the beneficial effects associated with these drugs in the treatment of muscle wasting of cachexia- or other age-related disorders. **(*Endocrinology* 154: 3764–3775, 2013)**

Ghrelin, a 28-amino acid peptide produced by the oxyntic cells of the stomach, is the endogenous ligand for the GH secretagogue receptor (GHS-R) type 1a (1). It has been proposed that ghrelin and GH secretagogues (GHSs) could be useful in some pathophysiological situations in which the hypothalamus-pituitary axis activity is impaired (2, 3). A growing number of studies highlight the possible therapeutic effects of these molecules in diseases associated with muscle wasting, including anorexia nervosa, chronic obstructive pulmonary disease, functional dyspepsia, and chronic heart failure (4–6), despite the necessity to assess the long-term efficacy and safety of GHSs therapies. Furthermore, the use of GHSs has been proposed to either prevent or treat the effects of aging and disuse on skeletal muscles (7–10). The synthesis of small peptides, pseudopeptides, and nonpeptidyl agonists to

ISSN Print 0013-7227 ISSN Online 1945-7170
Printed in U.S.A.

Received April 12, 2013. Accepted July 3, 2013.
First Published Online July 8, 2013

Abbreviations: CsA, cyclosporine A; EDL, extensor digitorum longus; GHS, GH secretagogue; GHS-R, GHS receptor; PLC, phospholipase C; PTP, permeability transition pore; SR, sarcoplasmic reticulum.

GHS-R1a has prompted novel approaches for their clinical use because such substances exhibit an equivalent efficacy to ghrelin and have a longer half-life and oral bioavailability (11–14). However, although the dose-response relationships of GHSs have been characterized with regard to their effects on GH and IGF-1 secretion, their extraendocrine effects have not been fully characterized. For example, it has been proposed that GHSs can increase lean body mass in aged subjects (9, 15), but studies focusing on their effects on muscle strength and physical performance revealed inconsistent results (8, 16). It should be noted that ghrelin and its mimetics can also act through mechanisms not mediated by GH; thus the effects of GHSs on multiple target tissues such as heart, skeletal muscle, fat, and bone could be correlated to the molecular structure of the GHS used. Chronic ghrelin administration in cachectic patients with chronic heart failure resulted in increased food intake and improved left ventricular dysfunction, suggesting that ghrelin effectively antagonizes muscle atrophy in humans (17, 18). However, it is widely known that the effects of ghrelin on the cardiovascular system are mediated by both GH-dependent and GH-independent mechanisms (19, 20). Ghrelin and hexarelin have been shown to directly affect sarcomere shortening, transient intracellular $Ca^{2+}$ levels, L-type $Ca^{2+}$ channel opening, and outward $K^+$ currents in isolated rat cardiomyocytes (21–23). Furthermore, ghrelin directly inhibits apoptosis of cardiomyocytes and endothelial cells through pathways involving kinase-172 and Akt serine kinase (24), whereas hexarelin protects rat cardiomyocytes from angiotensin II-induced apoptosis in vitro by modulating caspase activity and Bax/Bcl2 expression (25). Although the therapeutic potential of GHSs in the treatment of cachexia and muscular wasting is high (4, 5, 26), very little is known about the direct effects of peptidyl and nonpeptidyl GHSs on skeletal muscles. In previous studies, we documented that synthetic GHSs are capable of interfering with key processes involved in the excitability and excitation-contraction coupling of rat skeletal muscle (27). GHSs caused a decrease of resting chloride conductance, an electrical parameter modulated by the calcium-dependent protein kinase C. Because resting chloride conductance controls the electrical stability of sarcolemma (28, 29), this GHS-mediated effect could potentially produce an increase of muscle excitability and changes in the resistance to fatigue. Furthermore, in vitro application of GHSs caused a shift toward negative potentials of the mechanical threshold for contraction, which is a functional index of excitation-contraction coupling (27). These findings led us to hypothesize that GHSs could directly interfere with calcium machinery, a critical determinant of muscle function. In this context, tendon-to-tendon isolated skeletal muscle fibers were used to study drug effects in a cellular system with intact $Ca^{2+}$ signaling machinery. This study was performed to analyze the acute effects of ghrelin and synthetic GHSs on calcium homeostasis in isolated native skeletal muscle fibers and to elucidate the intracellular signaling pathway involved in these effects. Among the non-peptidyl-based structures, we studied the effects of the spiropiperidine derivative L163 255 (a structural analogue of the lead compound MK-0677) and the triazole derivative JMV2801, both of which have been extensively investigated in animal studies (12, 30–32), as well as the effects of JMV1843, a pseudopeptoid agonist of GHS-R1a. Ghrelin and hexarelin were chosen as the peptidyl GHSs. The use of the cell viability tetrazolium assay and molecular modeling allowed us to gain insight into the mechanism of action of GHSs on skeletal muscle as well as to define the molecular requisite for producing alterations in calcium homeostasis.

## Materials and Methods

### Animal care and surgery

Animal care and all experimental protocols involving animals were in accordance with the European Directive 2010/63/EU and were approved by the Italian Ministry of Health. Adult male Wistar rats (Charles River Laboratories, Calco, Italy) weighing 300–350 g were used. They had free access to food and tap water, were maintained at room temperature (22–24°C), and were exposed to a 12-hour light/12-hour dark cycle per day.

### Dissection of native muscle fibers

The extensor digitorum longus (EDL) muscle was removed from each animal under deep urethane anesthesia (1.2 g/kg body weight). Immediately after the surgery, the rats were maintained under anesthesia and euthanized with an anesthetic overdose. EDL muscles were pinned in a dissecting dish containing 95% $O_2$/5% $CO_2$-gassed normal physiological solution (the composition of which is defined later) at room temperature (22°C) for further dissection. Small bundles of 10–15 fibers arranged in a single layer were dissected lengthwise (tendon to tendon) with the use of microscissors, as previously described (33).

### Fura-2 fluorescence measurements in intact muscle fibers

Calcium measurements were performed using the membrane-permeable $Ca^{2+}$ indicator fura-2 acetoxymethyl ester (fura-2 AM, Molecular Probes-Invitrogen, Monza, Italy). Loading of muscle fibers was performed for 2 hours at 25°C in normal physiological solution containing 5 $\mu$M fura2-AM mixed to 0.05 % (vol/vol) Pluronic F-127 (Molecular Probes). After loading, muscle fibers were washed with normal physiological solution and mounted in a modified RC-27NE experimental chamber (Warner Instrument, Inc, Hamden, Connecticut) on the stage of an inverted Eclipse TE300 microscope (Nikon, Tokyo, Japan) with a 40× Plan-Fluor objective (Nikon). The mean sarcomere length

was set to 2.5–2.7 $\mu$m. Fluorescence measurements were made using a QuantiCell 900 integrated imaging system (Visitech International Ltd., Sunderland, UK) as previously described (33, 34).

During the experiments, pairs of background subtracted images of fura-2 fluorescence (510 nm) emitted after excitation at 340 and 380 nm were acquired and ratiometric images (340/380 nm) were calculated for each muscle fiber of the preparation using QC2000 software. Subsequently fluorescence ratio values were converted to the resting cytosolic calcium concentration, $[Ca^{2+}]_i$ (nM), after a calibration procedure using the following equation: $[Ca^{2+}]_i = (R - R_{min})/(R_{max} - R)*K_D*\beta$ where R is the ratio of the fluorescence emitted after excitation at 340 nm to the fluorescence after excitation at 380 nm; $K_D$ is the affinity constant of fura-2 for calcium, which was taken as 145 nM (Molecular Probes); and $\beta$ is a parameter according to Grynkiewicz et al. (35) that was determined experimentally in situ in ionomycin-permeabilized muscle fibers as previously described (33). $R_{min}$ and $R_{max}$ were determined in muscle fibers incubated in $Ca^{2+}$-free normal physiological solution containing 10 mM EGTA and in normal physiological solution, respectively. To check for fiber integrity, preparations were stimulated by the addition of 100 mM $K^+$ solution. Fibers that did not give rise to calcium transients after $K^+$ treatment were discarded.

## Determination of sarcolemmal permeability to divalent cations

The manganese quench technique was used to estimate the sarcolemmal permeability to divalent cations. $Mn^{2+}$ enters via the same routes as $Ca^{2+}$ but accumulates inside the cell. As $Mn^{2+}$ quenches the fluorescence of fura-2, the reduction of the fluorescence intensity can be used as an indicator of the time integral of $Mn^{2+}$ influx (36). Muscle preparations were perfused for 2 minutes with normal physiological solution containing 0.5 mM $MnCl_2$ as a surrogate of $CaCl_2$ (quenching solution). During the quenching protocol, the fluorescence emission of fura-2 excited at 360 nm was acquired at 1 Hz.

## Solution for fura-2 fluorescence measurements

The normal physiological solution was composed of 148 mM NaCl, 4.5 mM KCl, 2.5 mM $CaCl_2$, 1 mM $MgCl_2$, 0.44 mM $NaH_2PO_4$, 12 mM $NaHCO_3$, and 5.5 mM glucose. The pH of all solutions was adjusted to 7.3–7.4 by bubbling them with 95% $O_2$/5% $CO_2$. The calcium free-solution has the same composition as that of the normal physiological solution except that $CaCl_2$ was omitted and 10 mM EGTA was added. The quenching solution had the same composition except that 0.5 mM $MnCl_2$ was substituted for $CaCl_2$.

## Cell cultures and viability assay

C2C12 myocytes were cultured in DMEM supplemented with 10% fetal bovine serum, penicillin, streptomycin, and glutamine and were maintained at 37°C in 5% $CO_2$/95% air. Reportedly, C2C12 cells express the GHS-R1a (37, 38). Cell viability was assessed using the colorimetric [2-(2-methoxy-4-nitrophenyl)-3-(4-nitrophenyl)-5-(2,4-disulfophenyl)-2H-tetrazolium monosodium salt assay (cell counting kit, CCK8, Vinci-Biochem, Vinci, Italy) (39, 40). Cells were seeded in 96-well cultures at a density of approximately $1 \times 10^4$ cells per well and cultured for 18 hours to allow for attachment. The following day, the cells were treated with one of the test compounds (ghrelin, hexarelin, L163 255) dissolved in DMEM for 6 hours. Following exposure, 10 $\mu$L of [2-(2-methoxy-4-nitrophenyl)-3-(4-nitrophenyl)-5-(2,4-disulfophenyl)-2H-tetrazolium monosodium salt pure solution was added into each well, and then the plate was incubated for an additional 2 hours. The absorbance at 450 nm was measured using a spectrophotometer (microplate reader Victor V31420–40; PerkinElmer, Wellesley, Massachusetts). Cell viability (%) was expressed according to the following formula: cell viability (%) = [(test value-blank)/(control value-blank) $\times$ 100], where the blank value represents that of a cell-free well and the control value represents that of wells of cells treated with the vehicle alone (0.1% dimethysulfoxide).

## Molecular modeling study

The lowest energy conformers for each drug were searched using a systematic Merck Molecular Force Field analysis in the presence of water. A restricted number of conformers were found in the range of 3 kcal/mol on the basis of the Boltzmann distribution. The molecules were first constructed by fragments, and the molecular geometry was optimized to DFT B3LYP/6–31G* level theory and then submitted for a systematic Merck Molecular Force Field conformational analysis.

It was observed that the most populated low-energy conformer families were within the 3 kcal/mol range; among them, the lowest energy conformer was selected and used for the overlay. The conformers were superimposed at the level of the aminoacylamido groups and the near stereocenters with configuration R for the nonpeptidyl structures and JMV1843. The conformers were also superimposed at the same stereocenter and the amide bond for JMV1843 and hexarelin.

All calculations were performed with the SPARTAN '06 package (Wavefunction, Inc, Irvine, California) as described by Shao et al. (41) and using previously described calculation methods (42). Graphic representations and superimpositions were performed by Discovery Studio Modeling Environment, Release 3.5 (Accelrys, Inc., San Diego, California; 2005–2012).

## Determination of logD

The apparent pH-dependent distribution partition coefficients (logD) for dissociate mixtures of hexarelin, JMV 1843, JMV 2959, JMV 2810, and L163 255 were calculated by the online Advanced Chemistry Development, Inc. software I-Lab 2.0/LogD module (version 5.0.0.184, 2010–2013), as previously reported (43). The structures were drawn with the ACD/ChemSketch 12 freeware tool and submitted for online calculations to the ACD/I-Lab 2.0/LogD module at the website ilab.acdlabs.com. The logarithm of the apparent octanol-water partition coefficient D for all (including ionized) compound species at various pH values was calculated.

## Chemicals

All chemicals cited above as well as ionomycin, caffeine, cyclosporine A (CsA), thapsigargin, and U73122 were purchased from Sigma (St Louis, Missouri). Hexarelin, L163 255 (provided by Merck Research Laboratories, Rahway, New Jersey), JMV1843, JMV2810, and JMV2959 (a kind gift from Dr. Daniel Perrissoud, Aetherna-Zentaris, Frankfurt, Germany), as well as ghrelin (Tocris Cookson Ltd, Bristol, United Kingdom) and

[D-Lys-3]-GHRP-6 (Bachem AG, Bubendorf, Switzerland), were freshly dissolved in either normal or calcium-free physiological solution immediately prior to experimentation. Ghrelin, hexarelin, and L163 255 dosages for calcium imaging experiments and the tetrazolium assays evaluating cell viability were chosen based on previous studies (27, 37, 44–46).

### Statistical analysis

The data are presented as the mean ± SEM. One-way ANOVA, followed by Bonferroni's *t* test, was used to evaluate multiple statistical differences between groups. $P < .05$ was considered to be statistically significant.

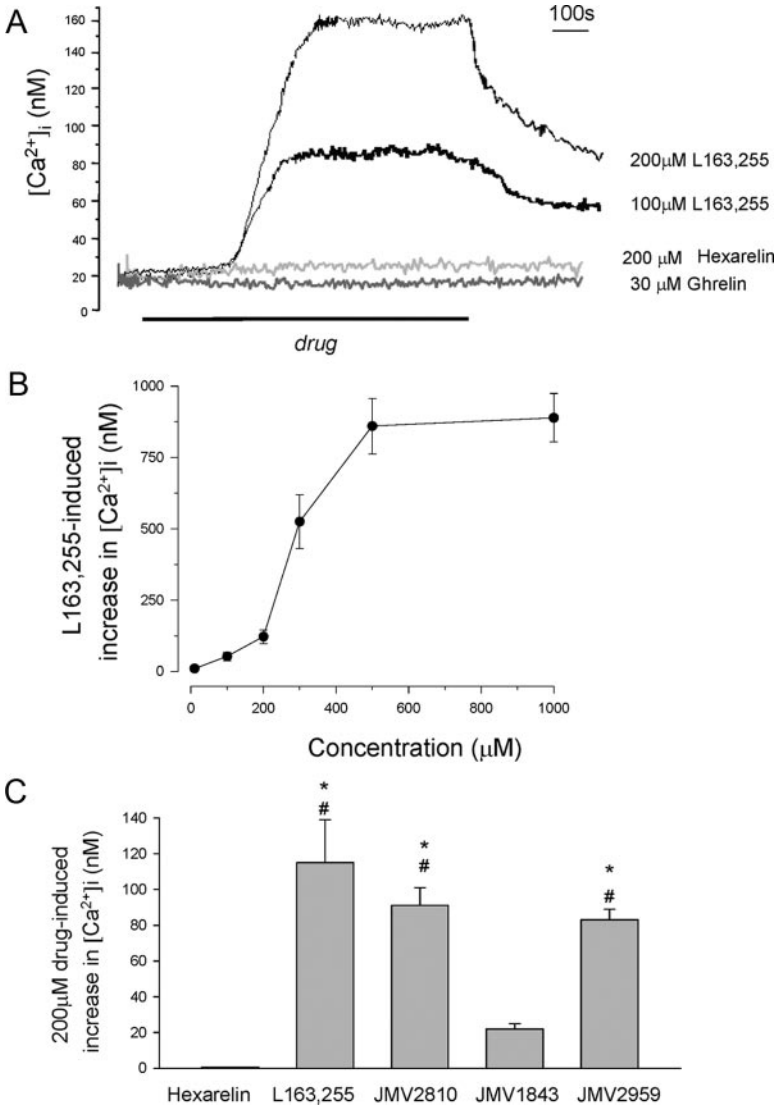


**Figure 1.** Effect of Peptidyl, Pseudopeptidyl, and Nonpeptidyl GHSs on $[Ca^{2+}]_i$ of Native Rat Skeletal Muscle Fibers. A, Representative traces of the typical calcium increase induced by the addition of either 100 or 200 $\mu$M L163 255 (black traces), as well as the lack of effect of hexarelin (gray trace) and ghrelin (light gray trace) on calcium homeostasis. B, Dose-response relationship for the effect of L163 255 on $[Ca^{2+}]_i$. The data are expressed as the mean ± SEM, and each point is representative of 18–25 fibers. C, Comparison of the effect induced by various GHSs at a concentration of 200 $\mu$M. Each bar represents the change of $[Ca^{2+}]_i$ induced by the indicated compound. The data are expressed as the mean ± SEM of 18–25 fibers. Statistical analysis by ANOVA showed significant differences ($F = 13$; $df = 4/81$; $P < .001$). Symbols represent statistically significant differences by the Bonferroni *t* test with respect to hexarelin (*) and JMV1843 (#) ($P < .05$ or less).

## Results

### Effect of GHSs on intracellular calcium homeostasis of native rat skeletal muscle fibers

#### *Peptidyl and nonpeptidyl GHSs differently affect $[Ca^{2+}]_i$ levels*

In accordance with previous studies (33, 34), resting $[Ca^{2+}]_i$ of fast-twitch EDL myofibers was in the 20–30 nM range. Representative traces showing the effects produced by the addition of each compound at the indicated tested concentrations are shown in Figure 1A. Doses of 1 nM, 300 nM, 1 $\mu$M, and 30 $\mu$M for the natural GHS ghrelin and the doses of 100 nM, 1 $\mu$M, 30 $\mu$M, and 200 $\mu$M for the peptidyl GHS hexarelin were used. At all of the indicated doses, neither ghrelin nor hexarelin affected resting calcium levels. In contrast to the peptidyl GHSs, the application of the nonpeptidyl spiropiperidine compound L163 255 caused a significant increase of $[Ca^{2+}]_i$. Treatment with 200 $\mu$M L163 255 led to an increase of $[Ca^{2+}]_i$ from 26 ± 3.9 nM to 144 ± 14 nM that was characterized by a slow rising phase and reached a plateau after 5 minutes (Figure 1A). The $[Ca^{2+}]_i$ increase continued during the entire drug exposure time of 15 minutes (data not shown). When the drug was removed, $[Ca^{2+}]_i$ significantly decreased (Figure 1A). The L163 255-induced increase of $[Ca^{2+}]_i$ was concentration dependent (Figure 1B). Similarly to L163 255, the nonpeptidyl triazole JMV2810 also induced a significant $[Ca^{2+}]_i$ increase. At a concentration of 200 $\mu$M, the JMV2810-induced $[Ca^{2+}]_i$ increase was almost superimposable on that induced by L163 255 (Figure 1C). The agonist L163 255 at the concentrations of 100 and 200 $\mu$M was selected for further investigations.

### L163 255-induced calcium increase is independent of GHS-R1a

The different effects mediated by peptidyl and nonpeptidyl GHSs on skeletal muscle calcium homeostasis

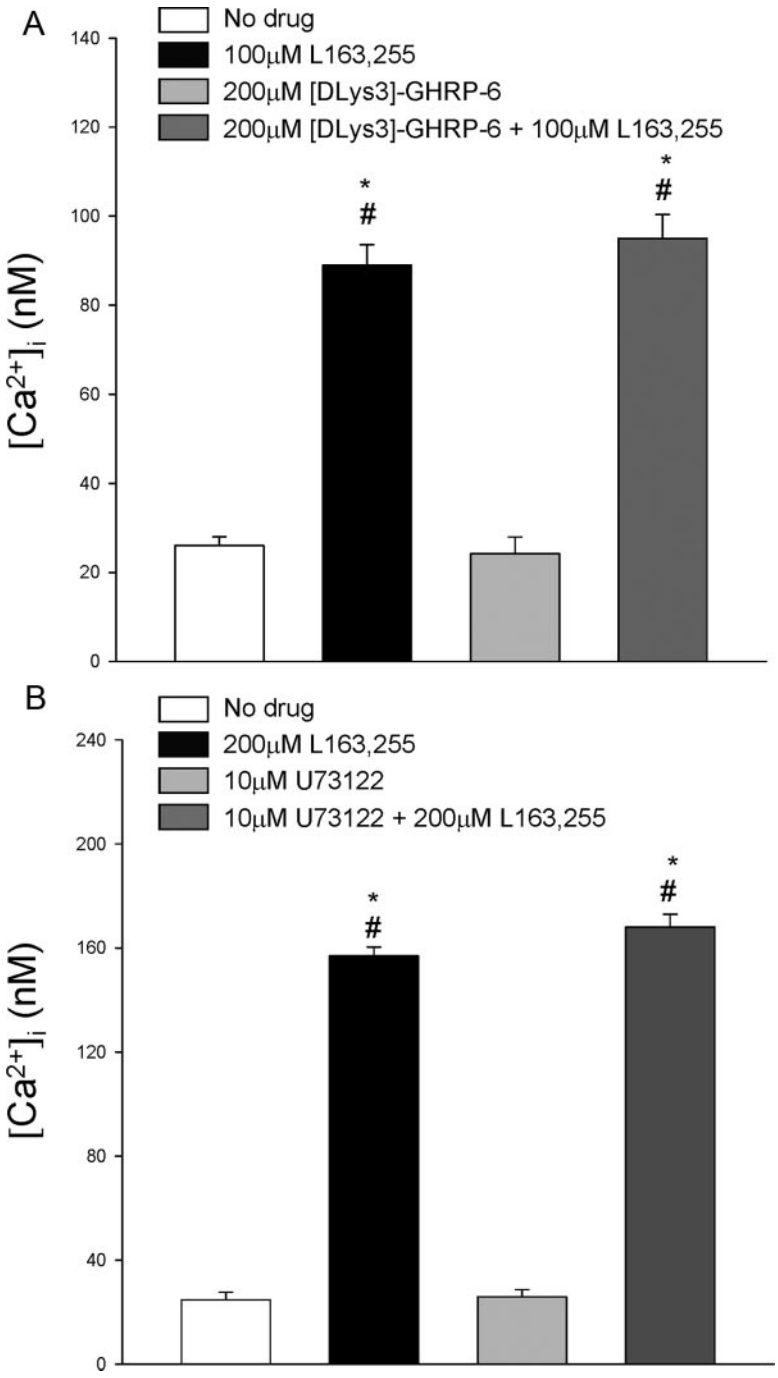


**Figure 2.** L163 255-Induced Calcium Increase Is Not Dependent on GHS-R1a. A, Effect of L163 255 in the presence of the GHS-R1a antagonist [D-Lys-3]-GHRP-6. The bars show the mean value of $[Ca^{2+}]_i$ from 10–20 fibers recorded in the absence and presence of L163 255 alone as well as after the addition of L163 255 to muscle fibers previously incubated with [D-Lys-3]-GHRP-6 for 20 minutes. The effect of [D-Lys-3]-GHRP-6 alone was also reported. The data are expressed as the mean ± SEM. Statistical analysis by ANOVA showed significant differences ($F = 86$; $df = 3/70$; $P < .001$). Symbols represent statistically significant differences by the Bonferroni *t* test with respect to no drug (*) and 200 μM [D-Lys-3]-GHRP-6 (#)($P < .05$ or less). B, Effect of L163 255 in the presence of the PLC inhibitor U73122. The bars show the mean value of $[Ca^{2+}]_i$ from 12–22 fibers recorded in the absence and presence of L163 255 alone as well as after the addition of L163 255 to muscle fibers previously incubated with U73122 for 20 minutes. The effect of U73122 alone was also reported. The data are expressed as the mean ± SEM. Statistical analysis by ANOVA showed significant differences ($F = 499$; $df = 3/71$; $P < .001$). Symbols represent statistically significant differences by the Bonferroni *t* test with respect to no drug (*)and 10 μM U73122 (#) ($P < .05$ or less).

led to the notion that the nonpeptidyl GHS-induced $[Ca^{2+}]_i$ increase was not mediated by activation of GHS-R1a. To test this hypothesis, specific inhibitors of GHS-R1a and of the downstream signaling pathway of this receptor were used. First, [D-Lys-3]-GHRP-6, shown to be a specific GHS-R1a competitive antagonist (3, 23, 47) was used. As shown in Figure 2A, the presence of 200 μM [D-Lys-3]-GHRP-6, which alone had no effect on resting $[Ca^{2+}]_i$, did not block the 100 μM L163 255-induced $[Ca^{2+}]_i$ increase. Phospholipase C (PLC) and phosphatidylinositol 3-kinase have been implicated in the signaling pathway of GHS-R1a (2, 23). Once again, preincubation with 10 μM U73122, a PLC inhibitor that by itself has no effect on resting $[Ca^{2+}]_i$, was unable to antagonize the effect of 200 μM L163 255 on $[Ca^{2+}]_i$ (Figure 2B).

## Investigation on the source of L163 255-induced calcium increase

We used the $Mn^{2+}$ quenching technique to assess the possibility that the L163 255-induced resting calcium increase in muscle fibers could be due to an increase in calcium influx. As shown in Figure 3, no modification of sarcolemmal permeability to divalent cations was observed after L163 255 treatment. The mean quench rate was 3.3 ± 0.2% $min^{-1}$ and 2.9 ± 0.3% $min^{-1}$ before and after the addition of 100 μM L163 255, respectively.

In accordance with the lack of effect on $Mn^{2+}$ permeability, the removal of external $Ca^{2+}$ in the bath solution did not abolish the L163 255-induced $[Ca^{2+}]_i$ increase, producing an increase of 115 ± 21 nM. This value was not significantly different from that obtained in the presence of extracellular calcium (Figure 4A). These results strongly suggest that the increase in $[Ca^{2+}]_i$

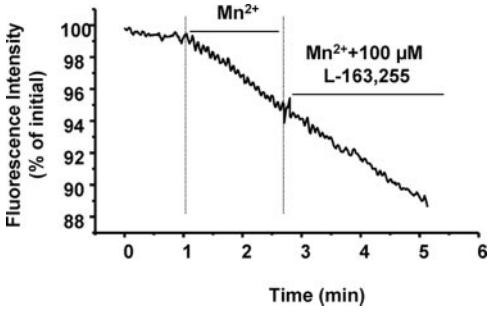


**Figure 3**. Lack of Effect of L163 255 on Sarcolemma Permeability to Divalent Cations. Typical recordings illustrating the effects of 100 $\mu$M L163 255 on Fura-2 fluorescence quenching associated with $Mn^{2+}$ ($MnCl_2$) influx in rat muscle fibers. The decline of Fura-2 fluorescence is expressed as the percentage per minute of initial fluorescence intensity. The quench rates were determined using linear regression analysis before and after treatment with L163 255, as reported in the text. Data are expressed as the mean ± SEM of 15–20 fibers.

induced by L163 255 is likely due to calcium release from intracellular stores. Thus, we attempted to identify the relevant intracellular sources. In Figure 4B, representative traces showing the L163 255-induced effects in the presence of various pharmacological tools are reported. Initially, we investigated the possible involvement of the sarcoplasmic reticulum (SR) using thapsigargin, which inhibits the $Ca^{2+}$-ATPase pump responsible for sequestering $Ca^{2+}$ in the SR and depletes the store by irreversibly preventing its refilling. After treatment with 10 $\mu$M thapsigargin, a double application of 40 mM caffeine allowed for SR $Ca^{2+}$ depletion (data not shown). When 200 $\mu$M L163 255 was successively applied to the same preparation, an increase of $[Ca^{2+}]_i$ was observed, although this increase was less intense than that observed in the control fibers (Figure 4, A and B). These data indicated that L163 255 partially mobilized $Ca^{2+}$ from the SR, but another intracellular calcium store was primarily involved. To rule out the possibility that this store was the mitochondria, we evaluated the effect of L163 255 in the presence of CsA, an inhibitor of the mitochondrial permeability transition pore (PTP) (34, 48). It is well known that mitochondria play a role in calcium homeostasis in skeletal muscle primarily by opening of PTP to induce a mitochondrial calcium efflux (49). In agreement with a previous study (34), the addition of 2 $\mu$M CsA did not alter the baseline of $[Ca^{2+}]_i$ (Figure 4B). A subsequent addition of 200 $\mu$M L163 255 to the CsA-treated fibers produced only a slight $[Ca^{2+}]_i$ increase (Figure 4, A and B). Thus, the CsA-mediated inhibition of the mitochondrial PTP significantly abolished the L163 255-induced $[Ca^{2+}]_i$ increase.

These findings indicate the partial involvement of the SR and primary involvement of mitochondria in the L163 255-induced alteration of calcium homeostasis in skeletal muscle fibers.

## Definition of the molecular requisite for nonpeptide GHS-induced calcium increase

To better define the different capabilities of the tested GHSs of interfering with the skeletal muscle $Ca^{2+}$ signaling machinery with regard to their chemical structure, the pseudopeptoid compound JMV1843 was tested. JMV1843 produced only a slight $[Ca^{2+}]_i$ increase, resulting in a less potent effect with respect to the nonpeptidyl compounds. Treatment with 200 $\mu$M JMV1843 stimulated a $[Ca^{2+}]_i$ increase of 19 ± 3.4 nM (Figure 1C). Furthermore, JMV 2959, a nonpeptidyl triazole derivative usually used as a potent GHS-R1a antagonist (50), also altered calcium homeostasis in a similar manner to that of the other tested nonpeptidyl GHS. When compared at a concentration of 200 $\mu$M (Figure 1C), JMV2959 induced a significant $[Ca^{2+}]_i$ increase that overlapped with those induced by L163 255 and JMV2810. These results were consistent with the conclusion that the chemical feature necessary for mediating a GHS-induced calcium increase is the nonpeptidyl structure.

## Effect of GHSs on cell viability of C2C12 skeletal muscle cells

Ghrelin and synthetic GHSs have been shown to exert different effects on proliferation and survival in human lung, prostate, skeletal muscle, breast carcinoma, and cancer cell lines (37, 44–46). It is well established that unregulated elevation in $[Ca^{2+}]_i$ may lead to cytotoxicity; thus the effects of peptidyl and nonpeptidyl GHSs on cell viability of C2C12 myoblasts were determined.

Ghrelin and the synthetic peptidyl hexarelin showed no effect on cell viability at any of the doses tested (Figure 5A). However, treatment with L163 255 significantly decreased the viability of C2C12 myocytes in a dose-dependent manner (Figure 5B). In the presence of 1, 10, 50, and 100 $\mu$M L163 255, cell viability was significantly decreased by 13 ± 2, 23 ± 3, 52 ± 3, and 96 ± 1%, respectively.

## Molecular modeling

To support the experimental observations and to identify the molecular determinants of GHSs likely to affect calcium homeostasis in native skeletal muscle, molecular modeling studies were carried out. Conformational search studies showed that all examined GHSs exhibit a restricted number of low-energy conformers. The lowest energy conformers of each compound are shown in Figure 6A. The molecular overlay between hexarelin and JMV1843 highlights the presence of the amide bond in JMV1843 that confers the nature of pseudopeptoid to this compound usually defined as a modified tripeptide derived by truncating hexarelin (13). The low-energy conformers of both

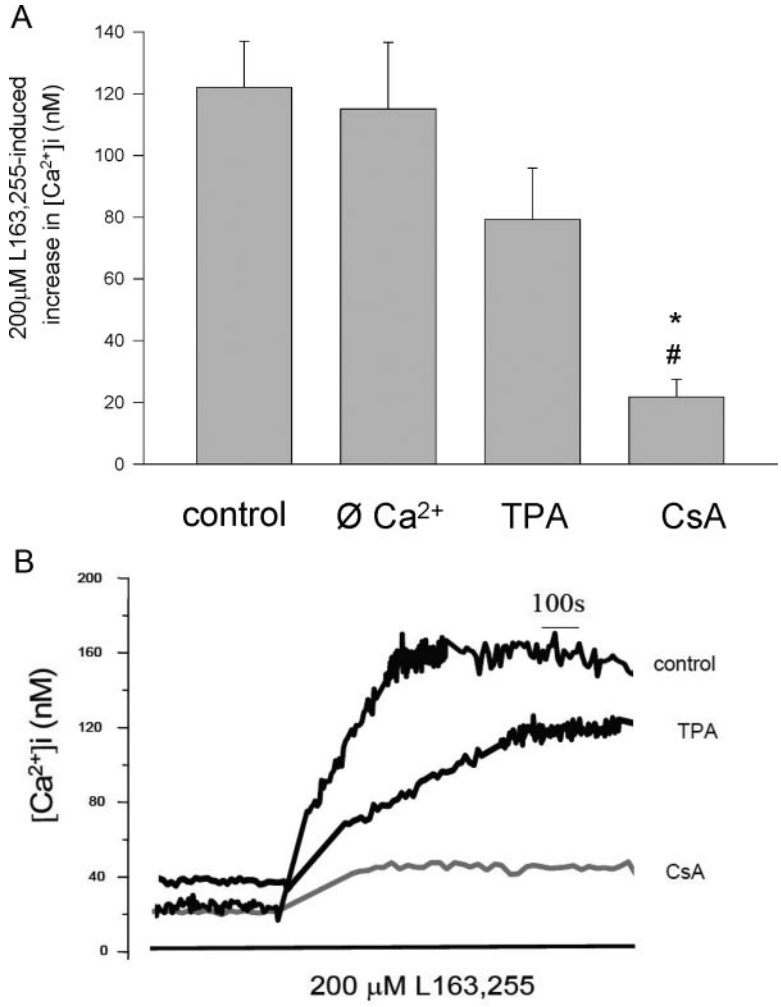


**Figure 4.** Investigation of the Calcium Source Responsible for the L163 255-Induced Increase of $[Ca^{2+}]_i$. A, Summary of the L163 255-induced response (200 $\mu$M) in the presence of external calcium (control, n = 20), in the absence of external calcium (Ø $Ca^{2+}$, n = 16), in the presence of thapsigargin (TPA, n = 18), and in the presence of CsA (n = 15) was reported. Each bar represents the mean ± SEM. Statistical analysis by ANOVA showed significant differences (F = 5; *df* = 3/95; $P < .005$). Symbols represent statistically significant differences by the Bonferroni *t* test with respect to control (*) and Ø $Ca^{2+}$ (#) ($P < .05$ or less). B, Superimposed traces showing the effect of the treatment with 200 $\mu$M L163 255 in the control condition, in the presence of the $Ca^{2+}$-ATPase inhibitor thapsigargin (TPA) (black trace), or in the presence of the mitochondrial PTP inhibitor CsA (gray trace). In the case of TPA, muscle fibers were incubated with 10 $\mu$M TPA for 15 minutes prior to repeated treatment with 40 mM caffeine, after which L163 255 was added. In the case of CsA, muscle fibers were incubated with 2 $\mu$M CsA for 10 minutes prior to the addition of L163 255.

molecules were characterized by the presence of intramolecular hydrogen bonds between the oxygen atom of the terminal formyl carbonyl group and the hydrogen atom on the amino group of the aminoacylamido group of the pseudopeptide amide bond for JMV1843 and between the terminal amino group of the histidine and the carboxamido oxygen atom of the alanine for hexarelin (Figure 6B).

Concerning the nonpeptidyl structures, all lower-energy conformer families exhibit the aromatic rings laying on different planes due to their molecular flexibility (Figure 6A). Particularly, an overlay of the lowest-energy conformers of L163 255, JMV2810, and JMV2959 indicated that all compounds displayed one overlapped spatially oriented aminoacyl group and 2 aromatic areas (Figure 6C). With respect to these nonpeptidyl GHSs, JMV1843 shared the aminoacyl group orientation but showed a differential spatial arrangement of the 2 aromatic areas. This latter conformational feature of JMV1843 could be due to the intramolecular hydrogen bonding, which is lacking in nonpeptidyl GHSs, that forces the indole aromatic rings into a more constrained configuration with respect to nonpeptidyl GHSs (Figure 6D).

### Lipophilicity

The peptide/nonpeptide structure of the GHSs influences their intrinsic physiochemical properties. The partition coefficient (logD) between octanol and aqueous solution at pH 7.4 of each of these compounds was determined as a measure of lipophilicity. Figure 7 shows the relationship of the logD value to drug-induced changes in calcium levels. Nonpeptidyl GHSs demonstrated a comparable capability of inducing $[Ca^{2+}]_i$ increase in skeletal muscle fibers and showed higher lipophilicity with respect to the peptide hexarelin, each with a logD value ranging from 2–4.

## Discussion

Numerous clinical trials involving both ghrelin agonists and antagonists in many type of diseases are currently underway. The primary area of interest involves the stimulation of appetite and fat accumulation by ghrelin and GHSs in wasting diseases and cachexia. However, a number of biological systems may be affected by these treatments as suggested by both the wide distribution of the cloned ghrelin receptor and a number of tissues and cell types known to respond to this hormone through a yet unidentified mechanism. Thus, the understanding of the diverse effects of GHSs on various tissues is pivotal to

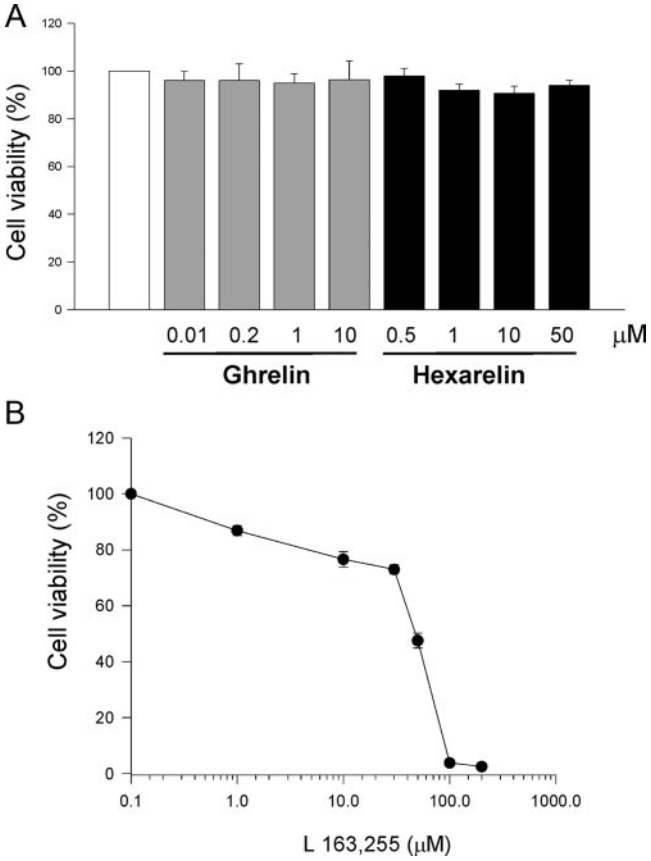


**Figure 5**. Effect of Peptidyl (Ghrelin, Hexarelin) and Nonpeptidyl (L163 255) GHSs on C2C12 Cell Viability as Determined by the Tetrazolium Assay. A, C2C12 cells were treated with either 0.01–10 $\mu$M ghrelin or 0.5–50 $\mu$M hexarelin using the incubation protocol described in *Materials and Methods*. The results are expressed as the percentage of the control and presented as the mean ± SEM. Each treatment had at least 10 replicates (wells). B, Dose-response relationship for the effect of L163 255 on cell viability. C2C12 cells were treated with 0.1–200 $\mu$M using the incubation protocol described in *Materials and Methods*. The results are expressed as the percentage of control and presented as the mean ± SEM. Each treatment had at least 10 replicates (wells). Statistical analysis by ANOVA showed no significant difference ($F = 1.79$).

develop specific and safe agonists and antagonists targeting the ghrelin system.

## Nonpeptidyl GHSs alter calcium homeostasis in skeletal muscle fibers

We demonstrated that GHSs affect skeletal muscle calcium homeostasis depending on their peptidyl or nonpeptidyl structure. Specifically, we showed for the first time that the synthetic nonpeptidyl GHSs under study were able to significantly increase $[Ca^{2+}]_i$ of native skeletal muscle fibers, whereas peptidyl GHSs did not affect calcium homeostasis. The pseudopeptoid JMV1843 produced only a slight increase of $[Ca^{2+}]_i$, further corroborating the hypothesis that the molecular requisite for mediating GHS-induced calcium alteration on skeletal muscle is the nonpeptidyl structure.

Given the pivotal role of calcium ions for muscle functionality, we identified the source of calcium involved in the non-peptidyl GHS-induced effects. The fact that the $[Ca^{2+}]_i$ rise produced in response to L163 255 occurred in the absence of external $Ca^{2+}$ demonstrated that the observed cytosolic calcium increase in skeletal muscle fibers resulted from intracellular calcium stores. The lack of effect of L163 255 in $Mn^{2+}$ quenching experiments also corroborated the involvement of $Ca^{2+}$ efflux from internal store in the drug mechanism of action. The reduced effect of L163 255 observed in the presence of either thapsigargin/caffeine or CsA led to the notion that the $[Ca^{2+}]_i$ increase was due to partial calcium release from the SR and primary release from the mitochondria.

It is widely known that excess $Ca^{2+}$ levels within cells are highly toxic, causing massive activation of proteases and several phospholipases. In various tissues, the PTP opening has been proposed as a likely candidate for $Ca^{2+}$-dependent effector of apoptosis (51). Accordingly, cell viability experiments on C2C12 cells suggested that nonpeptidyl GHSs triggered cell death.

## GHSs mechanism of action implications

In contrast to nonpeptidyl GHSs, ghrelin as well as the synthetic peptidyl GHS hexarelin did not alter calcium homeostasis or the viability of skeletal muscle fibers. These findings suggested that the effects of nonpeptidyl GHSs under study were likely not mediated by the cloned ghrelin receptor. Signaling from endogenous and synthetic GHSs is generally considered to occur through the GHS-R1a, and this receptor has been found in most tissues and organs of the body, including skeletal muscle (52, 53). By using [D-Lys-3]-GHRP-6 and U73122, we demonstrated that nonpeptidyl GHSs induced an increase in $[Ca^{2+}]_i$ through a mechanism that is independent from GHS-R1a activation. However, alternative binding sites for GHSs have been proposed in many types of tissues with different affinities toward the various GHS structures. It has been demonstrated that different GHS-R subtypes or receptor families are expressed in the cardiovascular tissues (54), and there are both similarities and differences between ghrelin and GHSs in terms of cardiac actions (20). All of the substances are able to increase cardiac performance either in animals or humans. However, in contrast to the nonpeptidyl GHSs, synthetic peptidyl GHSs and ghrelin itself are able to protect the heart from ischemia. This action appears to be mediated by a receptor specific to the synthetic peptidyl GHSs only (20). Also in our case, the differential GHS activity could be speculatively attributed to the different affinity of the GHSs to muscle-binding sites. However, based on the finding that JMV2959, a nonpeptide triazole derivative antagonist of GHS-R1a,

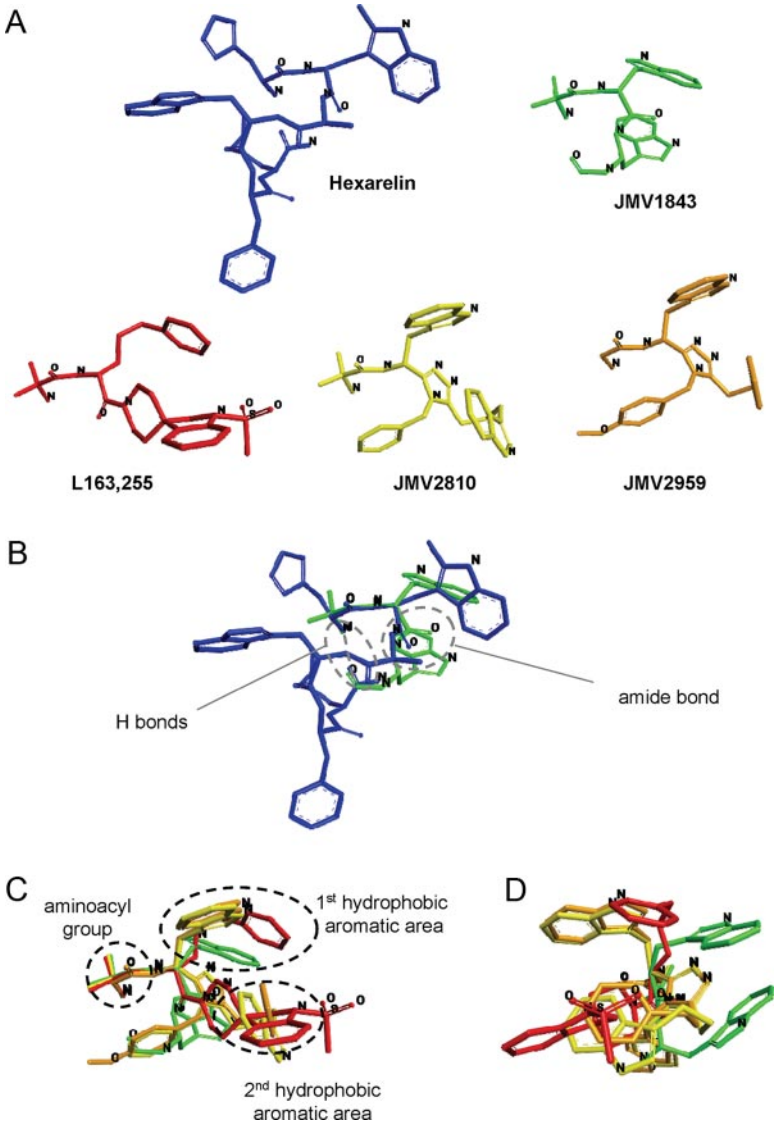


**Figure 6**. Modeling Study of GHSs. A, The lowest energy conformation of hexarelin, JMV1843, L163 255, JMV2810, and JMV2959 obtained as described in *Materials and Methods*. B, Overlay of the lowest energy conformations of the peptide hexarelin (blue) and pseudopeptoid JMV1843 (green). C, Overlay of the lowest energy conformations of the nonpeptides L163 255 (red), JMV2810 (yellow), and JMV2959 (orange) and the pseudopeptide JMV1843 (green). The fitting of the molecules was performed as described in *Materials and Methods*. D, 90° left rotation view of the molecules overlay described in panel C.

could induce a calcium increase as well as the postulated high capability of nonpeptidyl GHS crossing the plasma membrane due to their high molecular lipophilicity, we hypothesize that the observed effects on calcium homeostasis are due to a direct activation of an intracellular cascade by these nonpeptidyl GHSs.

## Modeling study

We attempted to explain the different effects of the GHSs on skeletal muscle calcium homeostasis by performing modeling investigations that allow us to compare the spatial geometry profiles associated with the tested peptide, pseudopeptoid, and nonpeptidyl GHSs. The most important conclusion is that all nonpeptidyl structures used have common spatial features. Indeed, overlaying the lowest-energy conformers of the nonpeptidyl structures, including the antagonist JMV2959, revealed that all of these compounds display 1 aminoacyl group and 2 hydrophobic aromatic areas similarly oriented.

Regarding nonpeptidyl GHSs, some interesting observations about the structure-calcium homeostasis alteration relationship may be drawn for peptidyl and pseudopeptoid structures. When the GHS type is correlated with the effect observed on skeletal muscle calcium homeostasis, it appears that JMV1843 represents a molecular switch with spatial conformational features between peptidyl and nonpeptidyl structures. Accordingly with the pseudopeptoid structure, the JMV1843 molecule contains an amide bond and an intramolecular hydrogen bond that overlay well with hexarelin. However, in comparison with the nonpeptidyl GHSs, the presence of an overlapped spatially oriented aminoacyl group and of the 2 aromatic areas in JMV1843 could contribute to the slight interference with calcium homeostasis. The different spatial orientations of the 2 aromatic areas with respect to L163 255 and JMV2810, most likely due to a more constrained configuration associated with JMV1843, could account for the reduced ability to induce increases in intracellular calcium levels with respect to nonpeptidyl GHS.

## Therapeutic implications and conclusions

Several studies have investigated the involvement of ghrelin and its analogues in wasting conditions, with promising results for therapeutic approaches (4, 6, 7). Wasting is defined as unintentional weight loss in which both fat-free mass and fat mass are lost, and it is characterized by severe malnutrition, weight loss, muscle atrophy, and anemia (55). Wasting is often the result of endocrine disorders accompanying the disease process itself.

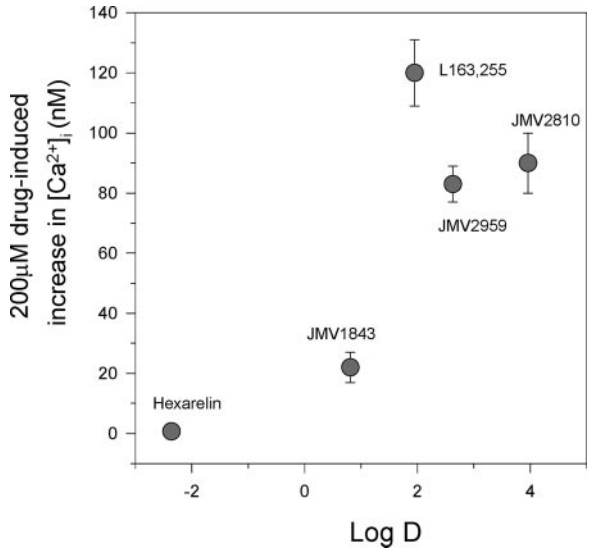


**Figure 7.** Relationship of GHS Lipophilicity and the Potency to Release $Ca^{2+}$ on Native Rat Skeletal Musclefibers. Each point represents the mean ± SEM of GHS-induced $[Ca^{2+}]_i$ increase at 200 $\mu$M (18–25 fibers) and the logD for each indicated derivative.

Among the hormonal mediators involved, ghrelin is a peptide that activates neurons of the arcuate nucleus of the hypothalamus, an area known to be important in the regulation of feeding. Regarding skeletal muscle, the continuous demand of efficacious treatment for several muscular degenerative pathologies, makes GHSs promising compounds with high therapeutic interest. Nonetheless, taking into account the wide spectrum of biological actions of GHS molecules, the assessment of the risk-benefit profile for this class of drugs is pivotal from both a therapeutic and toxicological point of view. Here, we demonstrated that the nonpeptidyl molecules L163 255 and JMV2810, but not the peptidyl molecules ghrelin and hexarelin, could affect calcium homeostasis and thus potentially exert detrimental effects on skeletal muscle functionality. The changes in calcium homeostasis induced by these nonpeptidyl GHSs may have multiple consequences that could exacerbate muscle damage. For example, it is widely known that calcium can stimulate muscle protein breakdown by increasing calpain and proteasome activity (56–58) as well as activate various transcription factors and nuclear cofactors that regulate gene transcription (59). From a pathophysiological point of view, changes in calcium homeostasis may be responsible for functional muscle loss. Accordingly, during aging, either in fast- or slow-twitch muscle fibers, the abnormally increased resting calcium concentration (60) induces the activation of $Ca^{2+}$-dependent proteases, which may contribute to sarcopenia and the clinically reported reduced muscle strength and exercise capacity typical of this condition. Thus, the nonpeptidyl GHSs under study could potentially exert direct effects on muscle functionality, which could counterbalance the beneficial effects associated with these drugs in the treatment of muscle wasting syndromes. Indeed, in cachexia and sarcopenia, the involvement of apoptosis though either DNA fragmentation or a significant calcium-dependent up-regulation of caspase activity appears to be widely proven (61, 62). It should be underlined that our data referred to the effect of some GHSs acutely applied in vitro. However, in vivo studies are needed to assess the detrimental effects on muscle functionality due to GHSs interference with calcium homeostasis. Further studies are also necessary to clarify whether the calcium-induced changes are a common feature of all nonpeptidyl GHSs. However, the effect of L163 255 on $[Ca^{2+}]_i$ and cell proliferation may provide a plausible link with the data reported by Bach et al. (63). MK-0677 treatment in older individuals who sustained a hip fracture did not produce clinically significant effects on physical function, although an increased in serum IGF-1 level was observed. In view of the molecular structure, it would be feasible that MK-0677, with a mechanism similar to that of the nonpeptidyl compounds used in this study, could affect calcium homeostasis and muscle function.

Furthermore, the lack of effects of the peptidyl GHSs on calcium homeostasis led us to define this class of GHSs as potentially safer than nonpeptidyl compounds. Also in this case, in vivo studies are needed to assess this hypothesis and to elucidate the clinical benefit associated with these molecules. Nevertheless, some previous in vivo studies do support our hypothesis. Indeed, according to the present results, the increase in expression of the 2 muscle-specific ubiquitin ligases, muscle RING-finger protein-1 (MuRF1) and atrogin-1/muscle atrophy F-box (MAFbx), seen in some models of cachexia and muscular wasting, was either normalized or prevented after the administration of ghrelin or peptidyl GHSs (38, 64, 65). Furthermore, it has been recently reported that in vivo ghrelin administration to animals and humans produced significant anticachectic effects (66–68). Any beneficial effect at these levels was reported with nonpeptidyl GHSs.

In summary, our study demonstrated that GHSs can differently affect skeletal muscle fibers depending on their molecular structure. The dysregulation in calcium homeostasis specifically induced by nonpeptidyl GHSs used in this study could potentially counterbalance the beneficial effects associated with these drugs in the treatment of muscle wasting in cachexia- or other age-related disorders.

## Acknowledgments

We thank Dr Antonia Scaramuzzi (Section of Pharmacology, Department of Pharmacy-Drug Sciences, University of Bari, Italy) for technical support with cytofluorimetric experiments.

Address all correspondence and requests for reprints to: Dr. Antonella Liantonio, Section of Pharmacology, Department of Pharmacy-Drug Sciences, University of Bari, Via Orabona, 4, Campus, I-70125 Bari, Italy. E-mail: antonella.liantonio@uniba.it.

This work was supported by a research grant from the Italian Space Agency (project Osteoporosis and Muscle Atrophy [OSMA]).

Disclosure Summary: The authors have nothing to disclose

## References


1. **Kojima M, Hosoda H, Date Y, Nakazato M, Matsuo H, Kangawa K.** Ghrelin is a growth-hormone-releasing acylated peptide from stomach. *Nature*. 1999;402:656–660.
2. **van der Lely AJ, Tschöp M, Heiman ML, Ghigo E.** Biological, physiological, pathophysiological, and pharmacological aspects of ghrelin. *Endocr Rev*. 2004;25:426–457.
3. **Smith RG, Jiang H, Sun Y.** Developments in ghrelin biology and potential clinical relevance. *Trends Endocrinol Metab*. 2005;16:436–442.
4. **Kamiji MM, Inui A.** The role of ghrelin and ghrelin analogues in wasting disease. *Curr Opin Clin Nutr Metab Care*. 2008;11:443–451.
5. **Akamizu T, Kangawa K.** Ghrelin for cachexia. *J Cachexia Sarcopenia Muscle*. 2010;1:169–176.
6. **Ueno H, Shiiya T, Nakazato M.** Translational research of ghrelin. *Ann NY Acad Sci*. 2010;1200:120–127.
7. **Ariyasu H, Iwakura H, Yamada G, Nakao K, Kangawa K, Akamizu T.** Efficacy of ghrelin as a therapeutic approach for age-related physiological changes. *Endocrinology*. 2008;149:3722–3728.
8. **Nass R, Pezzoli SS, Oliveri MC, et al.** Effects of an oral ghrelin mimetic on body composition and clinical outcomes in healthy older adults: a randomized trial. *Ann Intern Med*. 2008;149:601–611.
9. **White HK, Petrie CD, Landschulz W, et al.** Effects of an oral growth hormone secretagogue in older adults. *J Clin Endocrinol Metab*. 2009;94:1198–1206.
10. **Koshinaka K, Toshinai K, Mohammad A, et al.** Therapeutic potential of ghrelin treatment for unloading-induced muscle atrophy in mice. *Biochem Biophys Res Commun*. 2011;412:296–301.
11. **Broglio F, Boutignon F, Benso A, et al.** EP1572: a novel peptidomimetic GH secretagogue with potent and selective GH-releasing activity in man. *J Endocrinol Invest*. 2002;25:RC26–RC28.
12. **Smith RG.** Development of growth hormone secretagogues. *Endocr Rev*. 2005;26:346–360.
13. **Moulin A, Ryan J, Martinez J, Fehrentz JA.** Recent developments in ghrelin receptor ligands. *ChemMedChem*. 2007;2:1242–1259.
14. **Cordido F, Isidro ML, Nemiña R, Sangiao-Alvarellos S.** Ghrelin and growth hormone secretagogues, physiological and pharmacological aspect. *Curr Drug Discov Technol*. 2009;6:34–42.
15. **Svensson J, Ohlsson C, Jansson JO, et al.** Treatment with the oral growth hormone secretagogue MK-677 increases markers of bone formation and bone resorption in obese young males. *J Bone Miner Res*. 1998;13:1158–1166.
16. **Blackman MR.** Use of growth hormone secretagogues to prevent or treat the effects of aging: not yet ready for prime time. *Ann Intern Med*. 2008;149:677–679.
17. **Nagaya N, Moriya J, Yasumura Y, et al.** Effects of ghrelin administration on left ventricular function, exercise capacity, and muscle wasting in patients with chronic heart failure. *Circulation*. 2004;110:3674–3679.
18. **Cao JM, Ong H, Chen C.** Effects of ghrelin and synthetic GH secretagogues on the cardiovascular system. *Trends Endocrinol Metab*. 2006;17:13–18.
19. **Locatelli V, Rossoni G, Schweiger F, et al.** Growth hormone-independent cardioprotective effects of hexarelin in the rat. *Endocrinology*. 1999;140:4024–4031.
20. **Benso A, Broglio F, Marafetti L, et al.** Ghrelin and synthetic growth hormone secretagogues are cardioactive molecules with identities and differences. *Semin Vasc Med*. 2004;4:107–114.
21. **Xu XB, Cao JM, Pang JJ, et al.** The positive inotropic and calcium-mobilizing effects of growth hormone-releasing peptides on rat heart. *Endocrinology*. 2003;144:5050–5057.
22. **Sun Q, Ma Y, Zhang L, Zhao YF, Zang WJ, Chen C.** Effects of GH secretagogues on contractility and $Ca^{2+}$ homeostasis of isolated adult rat ventricular myocytes. *Endocrinology*. 2010;151:4446–4454.
23. **Sun Q, Zang WJ, Chen C.** Growth hormone secretagogues reduce transient outward K+ current via phospholipase C/protein kinase C signaling pathway in rat ventricular myocytes. *Endocrinology*. 2010;151:1228–1235.
24. **Baldanzi G, Filigheddu N, Cutrupi S, et al.** Ghrelin and des-acyl ghrelin inhibit cell death in cardiomyocytes and endothelial cells through ERK1/2 and PI 3-kinase/AKT. *J Cell Biol*. 2002;159:1029–1037.
25. **Pang JJ, Xu RK, Xu XB, et al.** Hexarelin protects rat cardiomyocytes from angiotensin II-induced apoptosis in vitro. *Am J Physiol Heart Circ Physiol*. 2004;286:H1063–H1069.
26. **DeBoer MD.** Ghrelin and cachexia: will treatment with GHSR-1a agonists make a difference for patients suffering from chronic wasting syndromes? *Mol Cell Endocrinol*. 2011;340:97–105.
27. **Pierno S, De Luca A, Desaphy JF, et al.** Growth hormone secretagogues modulate the electrical and contractile properties of rat skeletal muscle through a ghrelin-specific receptor. *Br J Pharmacol*. 2003;139:575–584.
28. **Pedersen TH, de Paoli F, Nielsen OB.** Increased excitability of acidified skeletal muscle: role of chloride conductance. *J Gen Physiol*. 2005;125:237–246.
29. **Burge, JA, Hanna MG.** Novel insights into the pathomechanisms of skeletal muscle channelopathies. *Curr Neurol Neurosci Rep*. 2012;12:62–69.
30. **Demange L, Boeglin D, Moulin A, et al.** Synthesis and pharmacological in vitro and in vivo evaluations of novel triazole derivatives as ligands of the ghrelin receptor. 1. *J Med Chem*. 2007;50:1939–1957.
31. **Moulin A, Demange L, Bergé G, et al.** Toward potent ghrelin receptor ligands based on trisubstituted 1,2,4-triazole structure. 2. Synthesis and pharmacological in vitro and in vivo evaluations. *J Med Chem*. 2007;50:5790–5806.
32. **Bresciani E, Tamiazzo L, Torsello A, et al.** Ghrelin control of GH secretion and feeding behaviour: the role of the GHS-R1a receptor studied in vivo and in vitro using novel non-peptide ligands. *Eat Weight Disord*. 2008;13:e67–e74.
33. **Fraysse B, Desaphy JF, Pierno S, et al.** Decrease in resting calcium and calcium entry associated with slow-to-fast transition in unloaded rat soleus muscle. *FASEB J*. 2003;17:1916–1918.
34. **Liantonio A, Giannuzzi V, Cippone V, Camerino GM, Pierno S, Camerino DC.** Fluvastatin and atorvastatin affect calcium homeostasis of rat skeletal muscle fibers in vivo and in vitro by impairing the sarcoplasmic reticulum/mitochondria Ca2+-release system. *J Pharmacol Exp Ther*. 2007;321:626–634.
35. **Grynkiewicz G, Poenie M, Tsien RY.** A new generation of $Ca^{2+}$ indicators with greatly improved fluorescence properties. *J Biol Chem*. 1985;260:3440–3450.
36. **Parekh AB, Penner R.** Store depletion and calcium influx. *Physiol Rev*. 1997;77:901–930.
37. **Filigheddu N, Gnocchi VF, Coscia M, et al.** Ghrelin and des-acyl ghrelin promote differentiation and fusion of C2C12 skeletal muscle cells. *Mol Biol Cell*. 2007;18:986–994.

38. **Yamamoto D, Ikeshita N, Matsubara T, et al.** GHRP-2, a GHS-R agonist, directly acts on myocytes to attenuate the dexamethasone-induced expressions of muscle-specific ubiquitin ligases, Atrogin-1 and MuRF1. *Life Sci*. 2008;82:460–466.
39. **Berridge MV, Herst PM, Tan AS.** Tetrazolium dyes as tools in cell biology: new insights into their cellular reduction. *Biotechnol Annu Rev*. 2005;11:127–152.
40. **Ogura T, Tanaka Y, Nakata T, Namikawa T, Kataoka H, Ohtsubo Y.** Simvastatin reduces insulin-like growth factor-1 signaling in differentiating C2C12 mouse myoblast cells in an HMG-CoA reductase inhibition-independent manner. *J Toxicol Sci*. 2007;32:57–67.
41. **Shao Y, Molnar LF, Jung Y, et al..** Advances in methods and algorithms in a modern quantum chemistry program package. *Phys Chem Chem Phys*. 2006;8:3172–3191.
42. **Hehre WJA.** *Guide to Molecular Mechanics and Quantum Chemical Calculations*, 2nd ed. Irvine, CA: Wavefunction Inc; 2006
43. **Bhal SK, Kassam K, Peirson IG, Pearl GM.** The Rule of Five revisited: applying log D in place of log P in drug-likeness filters. *Mol Pharm*. 2007;4:556–560.
44. **Ghè C, Cassoni P, Catapano F, et al.** The antiproliferative effect of synthetic peptidyl GH secretagogues in human CALU-1 lung carcinoma cells. *Endocrinology*. 2002;143:484–491.
45. **Cassoni P, Ghé C, Marrocco T, et al.** Expression of ghrelin and biological activity of specific receptors for ghrelin and des-acyl ghrelin in human prostate neoplasms and related cell lines. *Eur J Endocrinol*. 2004;150:173–184.
46. **Jeffery PL, Herington AC, Chopin LK.** Expression and action of the growth hormone releasing peptide ghrelin and its receptor in prostate cancer cell lines. *J Endocrinol*. 2002;172:R7–R11.
47. **Traebert M, Riediger T, Whitebread S, Scharrer E, Schmid HA.** Ghrelin acts on leptin-responsive neurones in the rat arcuate nucleus. *J Neuroendocrinol*. 2002;14:580–586.
48. **Crompton M, Virji S, Doyle V, Johnson N, Ward JM.** The mitochondrial permeability transition pore. *Biochem Soc Symp*. 1999; 66:167–179.
49. **Saris NE, Carafoli E.** A historical review of cellular calcium handling, with emphasis on mitochondria. *Biochemistry (Mosc)*. 2005; 70:187–194.
50. **Moulin A, Brunel L, Boeglin D, et al.** The 1,2,4-triazole as a scaffold for the design of ghrelin receptor ligands: development of JMV 2959, a potent antagonist. *Amino Acids*. 2013;44:301–314.
51. **Rimessi A, Giorgi C, Pinton P, Rizzuto R.** The versatility of mitochondrial calcium signals: from stimulation of cell metabolism to induction of cell death. *Biochim Biophys Acta*. 2008;1777:808–816.
52. **Papotti M, Ghè C, Cassoni P, et al.** Growth hormone secretagogue binding sites in peripheral human tissues. *J Clin Endocrinol Metab*. 2000;85:3803–3807.
53. **Gnanapavan S, Kola B, Bustin SA, et al.** The tissue distribution of the mRNA of ghrelin and subtypes of its receptor, GHS-R, in humans. *J Clin Endocrinol Metab*. 2002;87:2988–2991.
54. **Muccioli G, Baragli A, Granata R, Papotti M, Ghigo E.** Heterogeneity of ghrelin/growth hormone secretagogue receptors. Toward the understanding of the molecular identity of novel ghrelin/GHS receptors. *Neuroendocrinology*. 2007;86:147–164.
55. **Kulstad R, Schoeller DA.** The energetics of wasting diseases. *Curr Opin Clin Nutr Metab Care*. 2007;10:488–493.
56. **Menconi MJ, Wei W, Yang H, Wray CJ, Hasselgren PO.** Treatment of cultured myotubes with the calcium ionophore A23187 increases proteasome activity via a CaMK II-caspase-calpain-dependent mechanism. *Surgery*. 2004;136:135–142.
57. **Costelli P, Reffo P, Penna F, Autelli R, Bonelli G, Baccino FM.** Ca(2+)-dependent proteolysis in muscle wasting. *Int J Biochem Cell Biol*. 2005;37:2134–2146.
58. **Fareed MU, Evenson AR, Wei W, et al.** Treatment of rats with calpain inhibitors prevents sepsis-induced muscle proteolysis independent of atrogin-1/MAFbx and MuRF1 expression. *Am J Physiol Regul Integr Comp Physiol*. 2006;290:R1589–R1597.
59. **Berridge MJ, Bootman MD, Roderick HL.** Calcium signalling: dynamics, homeostasis and remodelling. *Nat Rev Mol Cell Biol*. 2003; 4:517–529.
60. **Fraysse B, Desaphy JF, Rolland JF, et al.** Fiber type-related changes in rat skeletal muscle calcium homeostasis during aging and restoration by growth hormone. *Neurobiol Dis*. 2006;21:372–380.
61. **Hasselgren PO, Fischer JE.** Muscle cachexia: current concepts of intracellular mechanisms and molecular regulation. *Ann Surg*. 2001;233:9–17.
62. **Gissel H.** The role of Ca2+ in muscle cell damage. *Ann NY Acad Sci*. 2005;1066:166–180.
63. **Bach MA, Rockwood K, Zetterberg C, et al.** The effects of MK-0677, an oral growth hormone secretagogue, in patients with hip fracture. *J Am Geriatr Soc*. 2004;52:516–523.
64. **Balasubramaniam A, Joshi R, Su C, et al.** Ghrelin inhibits skeletal muscle protein breakdown in rats with thermal injury through normalizing elevated expression of E3 ubiquitin ligases MuRF1 and MAFbx. *Am J Physiol Regul Integr Comp Physiol*. 2009;296:R893–R901.
65. **Sheriff S, Joshi R, Friend LA, James JH, Balasubramaniam A.** Ghrelin receptor agonist, GHRP-2, attenuates burn injury-induced MuRF-1 and MAFbx expression and muscle proteolysis in rats. *Peptides*. 2009;30:1909–1913.
66. **Miki K, Maekura R, Nagaya N, et al.** Ghrelin treatment of cachectic patients with chronic obstructive pulmonary disease: a multicenter, randomized, double-blind, placebo-controlled trial. *PLoS One*. 2012;7:e35708.
67. **Matsumoto N, Nakazato M.** Clinical application of ghrelin for chronic respiratory diseases. *Methods Enzymol*. 2012;514:399–407.
68. **Porporato PE, Filigheddu N, Reano S, et al.** Acylated and unacylated ghrelin impair skeletal muscle atrophy in mice. *J Clin Invest*. 2013; 123:611–622.